

## Supplementary Information

### Computational design of a polymorph of 2D III-V orthorhombic monolayer by first principles calculation: Excellent anisotropic electronic and optical properties

Jun Zhao<sup>a,c,\*</sup>, Hui Zeng<sup>b,d,\*</sup>, Ge Yao<sup>e</sup>

<sup>a</sup> *New Energy Technology Engineering Laboratory of Jiangsu Province & School of Science, Nanjing University of Posts and Telecommunications, Nanjing 210023, China*

<sup>b</sup> *School of Electronic and Optical Engineering, Nanjing University of Science and Technology, Nanjing, Jiangsu 210094, China*

<sup>c</sup> *Department of Physics, University of Illinois at Urbana-Champaign, Urbana, IL61801, USA*

<sup>d</sup> *Holonyak Micro and Nanotechnology Lab, University of Illinois at Urbana-Champaign, Urbana, IL 61801, USA*

<sup>e</sup> *National Laboratory of Solid State Microstructures, Collaborative Innovation Center of Advanced Microstructures, Nanjing University, Nanjing 210093, China*

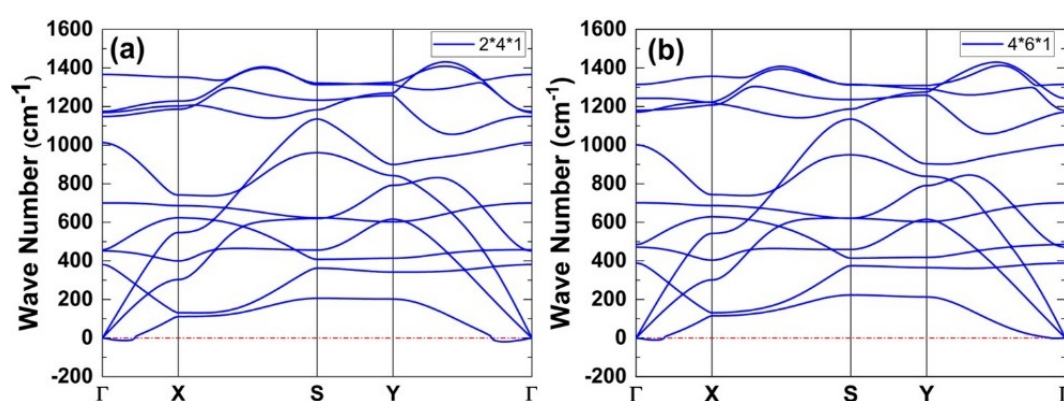


FIG. S1 The calculated phonon dispersion of the 2D orthorhombic BN monolayer by using different supercells.

\* Corresponding author. E-mail address: zhaojun@njupt.edu.cn

\* Corresponding author. E-mail address: zenghui@njust.edu.cn

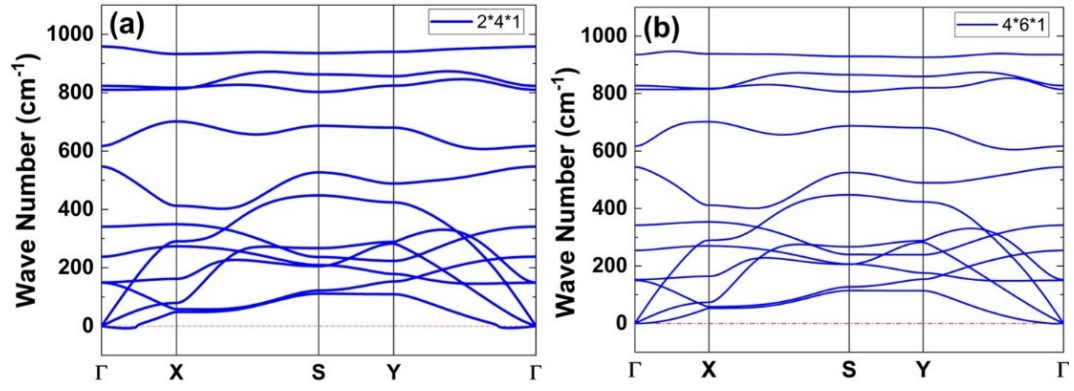


FIG. S2 The calculated phonon dispersion of the 2D orthorhombic AlN by using different supercells.

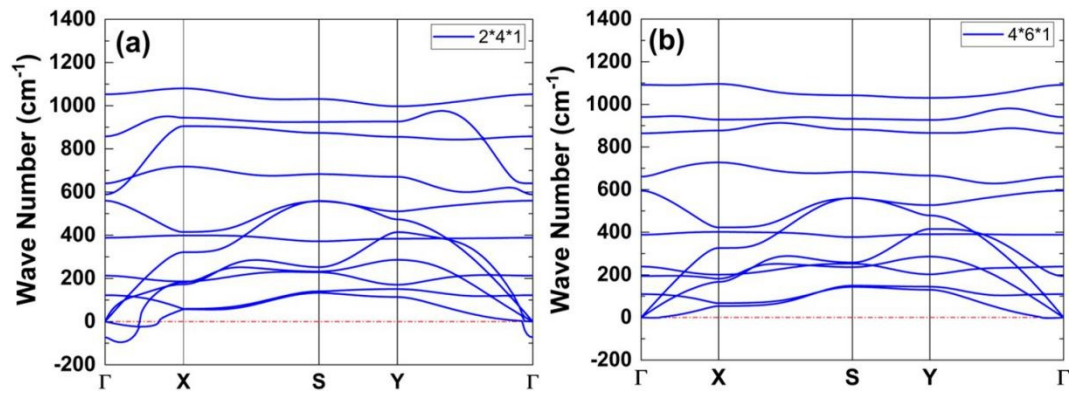


FIG. S3 The calculated phonon dispersion of the 2D orthorhombic BP by using different supercell

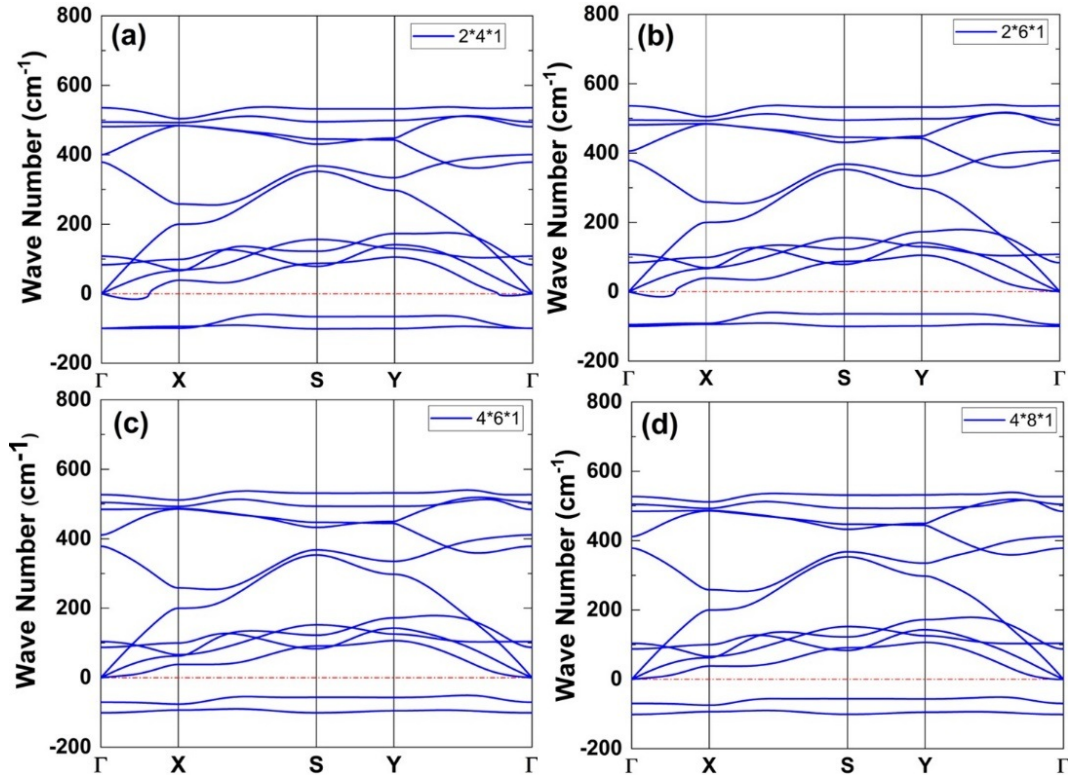


FIG. S4 The calculated phonon dispersion of the 2D orthorhombic AIP by using different supercells.

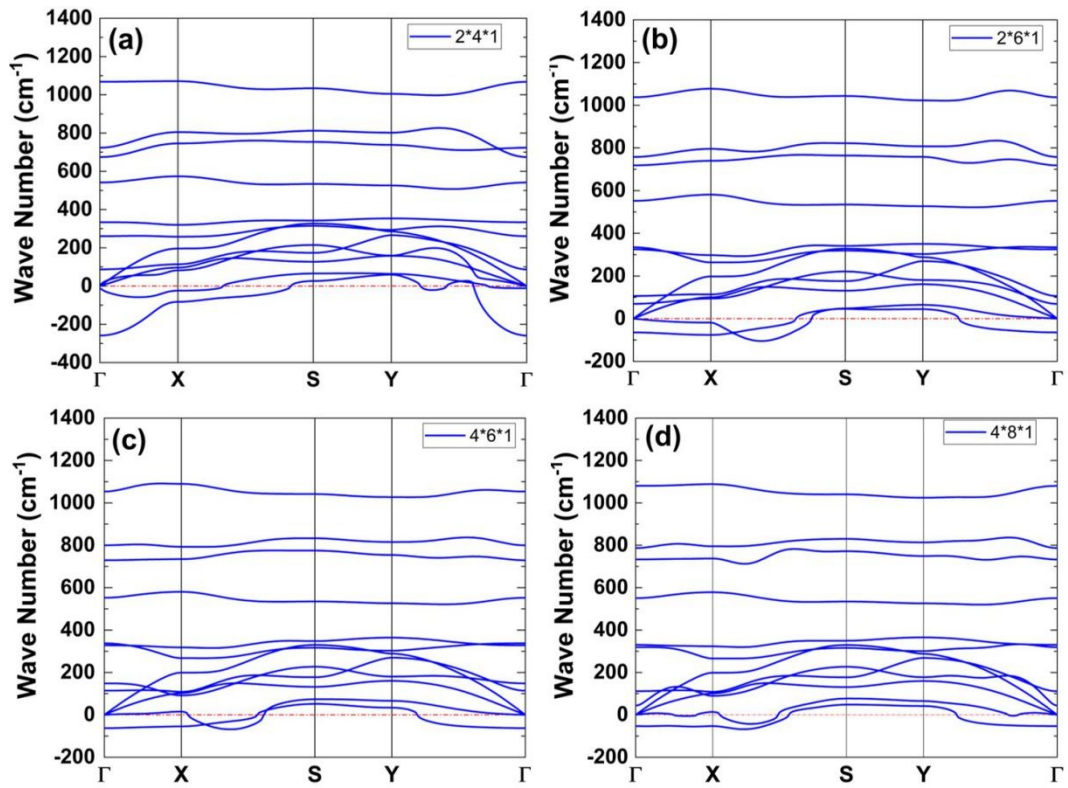


FIG. S5 The calculated phonon dispersion of the 2D orthorhombic BAs by using different supercells.

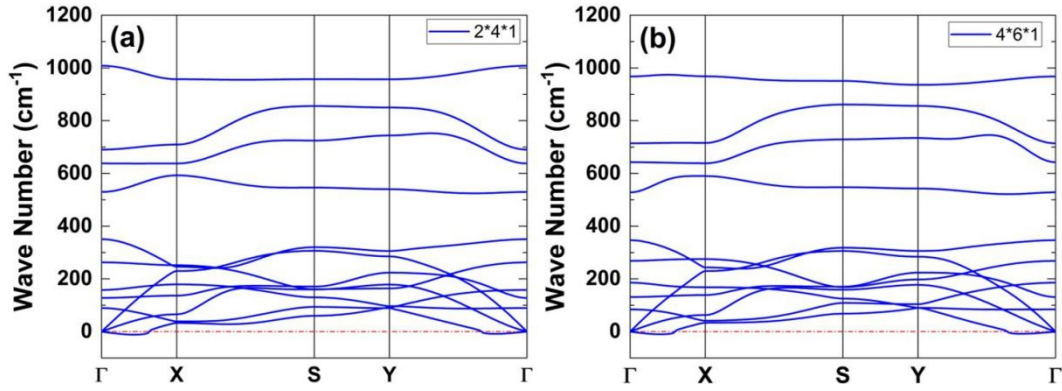


FIG. S6 The calculated phonon dispersion of the 2D orthorhombic GaN by using different supercells.

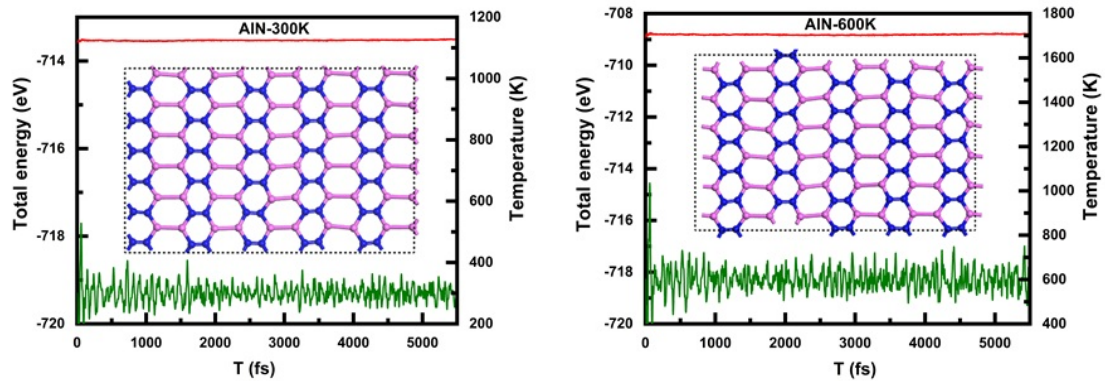


FIG. S7 The calculated AIMD results of the 2D orthorhombic AlN monolayer at 300K (left column) and 600K (right column). The temperature and the total energy curves with respect to time are shown by green and red lines, respectively. The inset shows the snapshot of final atomic structure at 5.5 ps.

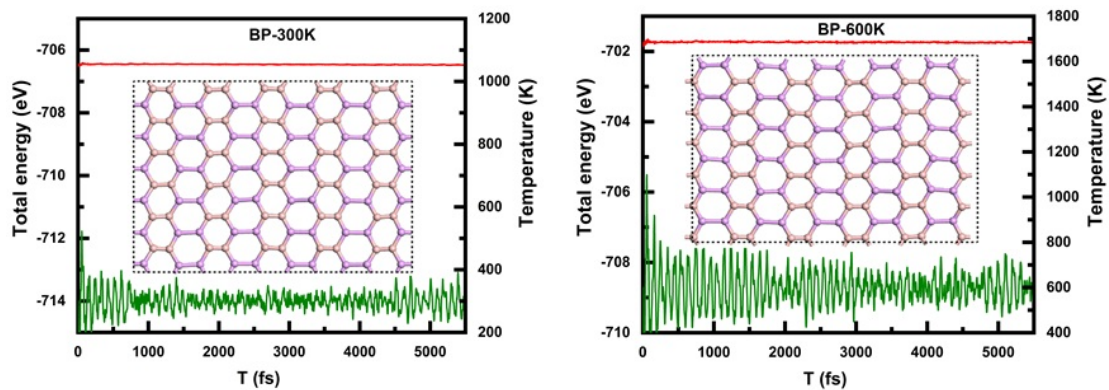


FIG. S8 The calculated AIMD results of the 2D orthorhombic BP monolayer at 300K (left column) and 600K (right column). The temperature and the total energy curves with respect to time are shown by green and red lines, respectively. The inset shows the snapshot of final atomic structure at 5.5 ps.

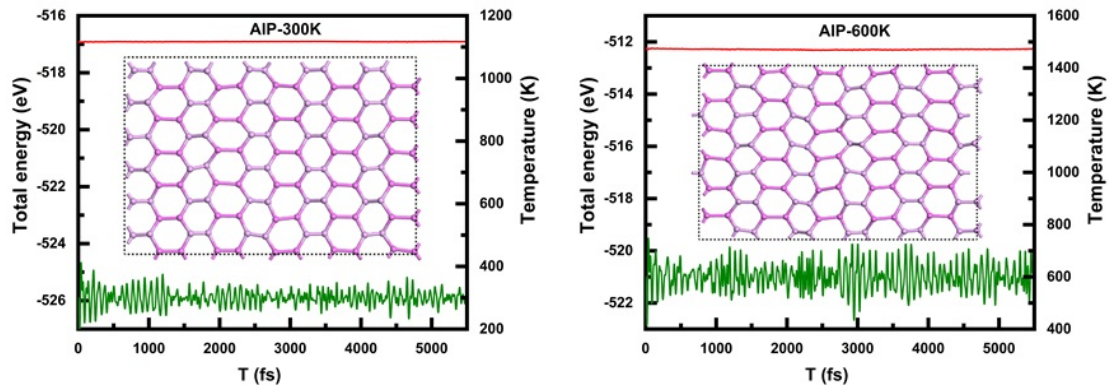


FIG. S9 The calculated AIMD results of the 2D orthorhombic AIP monolayer at 300K (left column) and 600K (right column). The temperature and the total energy curves with respect to time are shown by green and red lines, respectively. The inset shows the snapshot of final atomic structure at 5.5 ps.

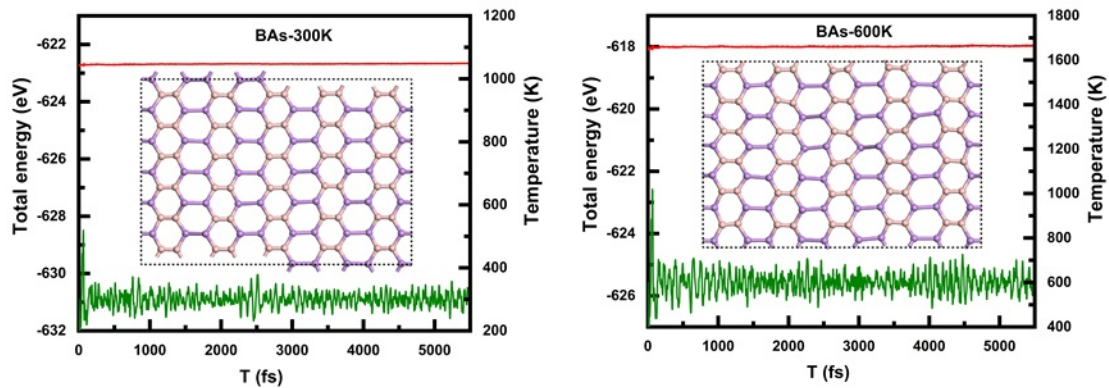


FIG. S10 The calculated AIMD results of the 2D orthorhombic BAs monolayer at 300K (left column) and 600K (right column). The temperature and the total energy curves with respect to time are shown by green and red lines, respectively. The inset shows the snapshot of final atomic structure at 5.5 ps.

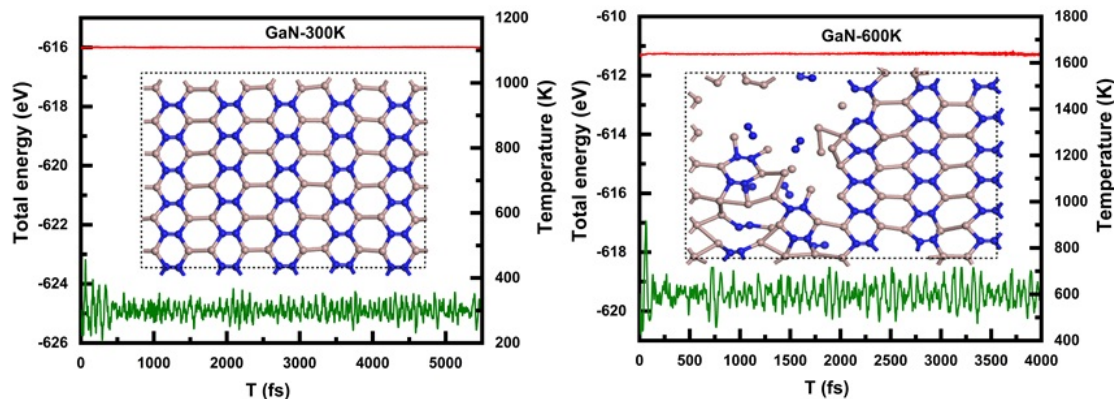


FIG. S11 The calculated AIMD results of the 2D orthorhombic GaN monolayer at 300K (left column) and 600K (right column). The temperature and the total energy curves with respect to time are shown by green and red lines, respectively. The inset shows the snapshot of final atomic structure at 5.5 ps and 4 ps for 300 and 600 K, respectively.

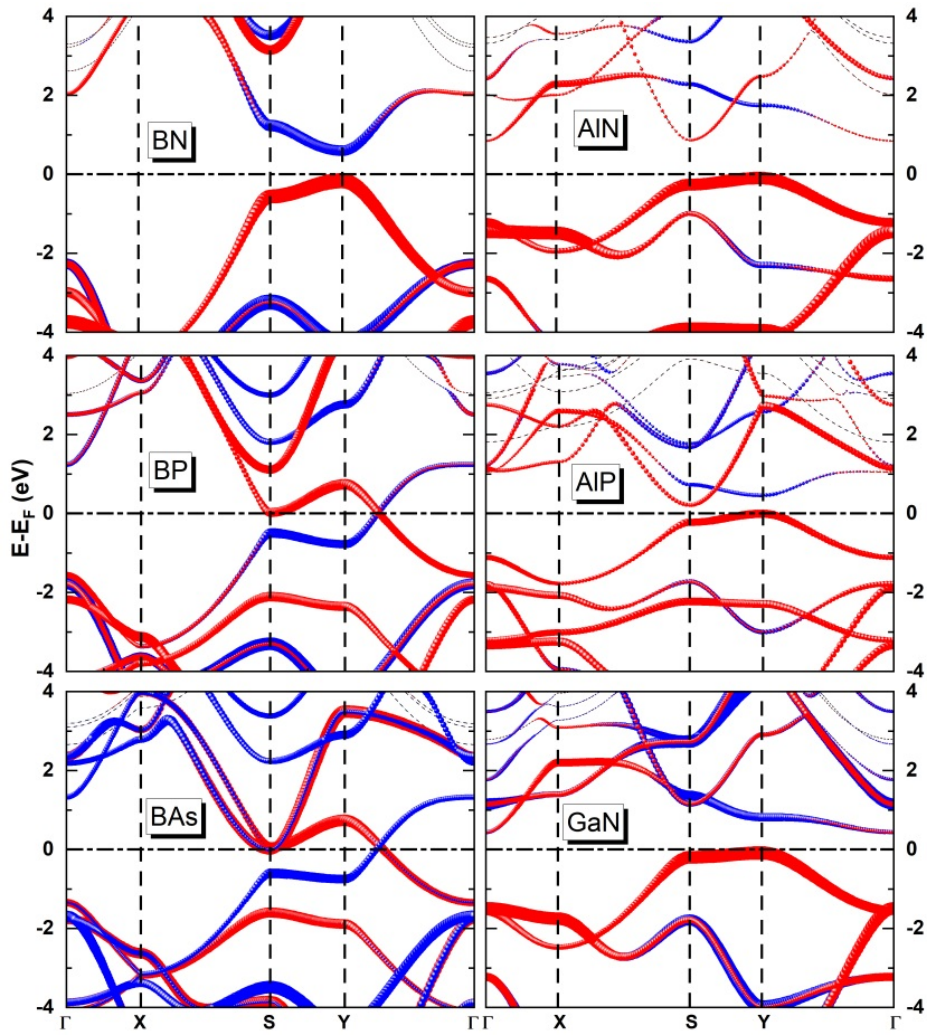


FIG. S12 The calculated electronic band structure results of the 2D III-V orthorhombic monolayers by using GGA-PBE potential. The contributions from group-III atom and group-V atom are denoted by blue and red circles, respectively

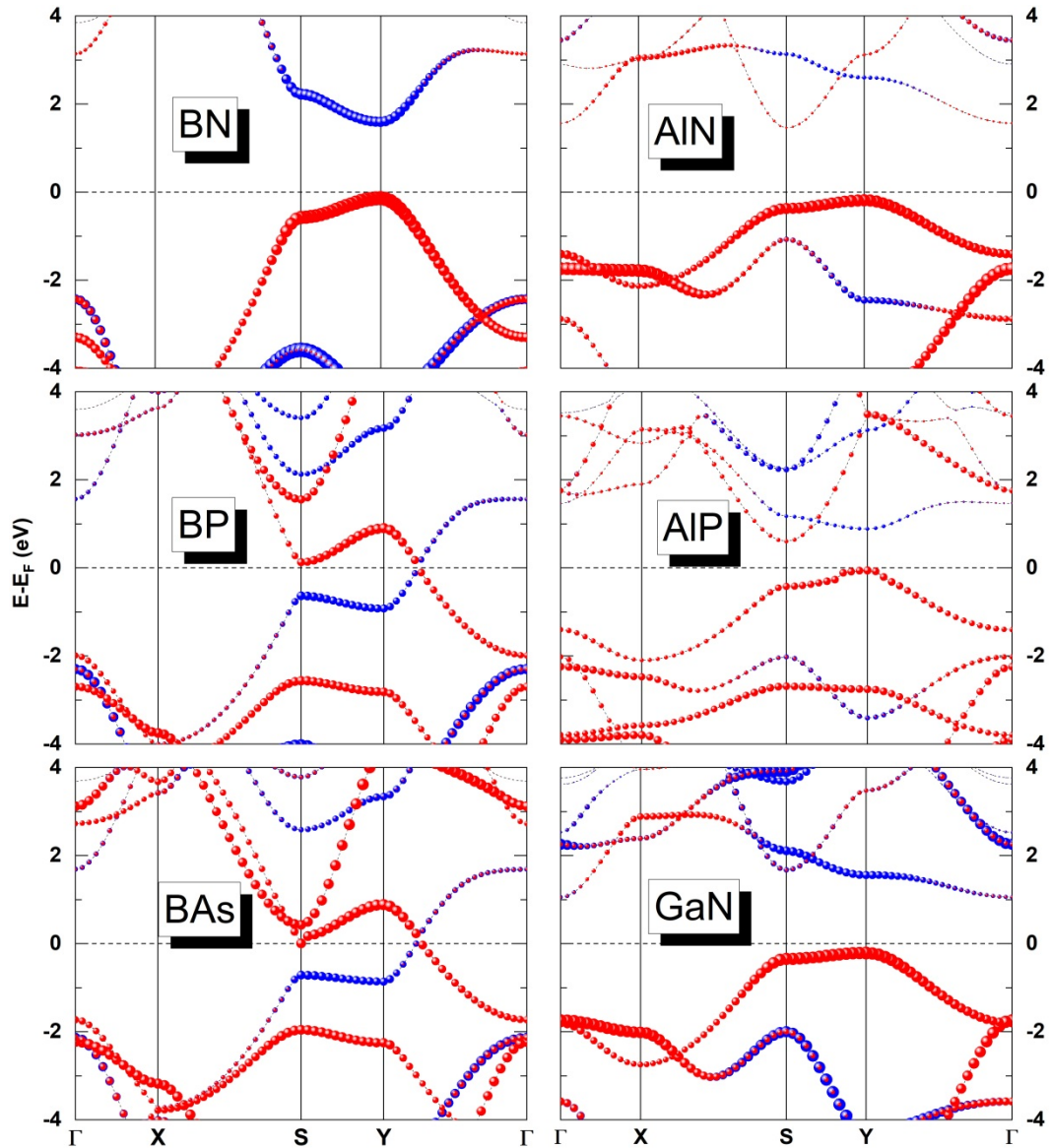


FIG. S13 The calculated electronic band structure results of the 2D III-V orthorhombic monolayers by using HSE potential. The contributions from group-III atom and group-V atom are denoted by blue and red circles, respectively.

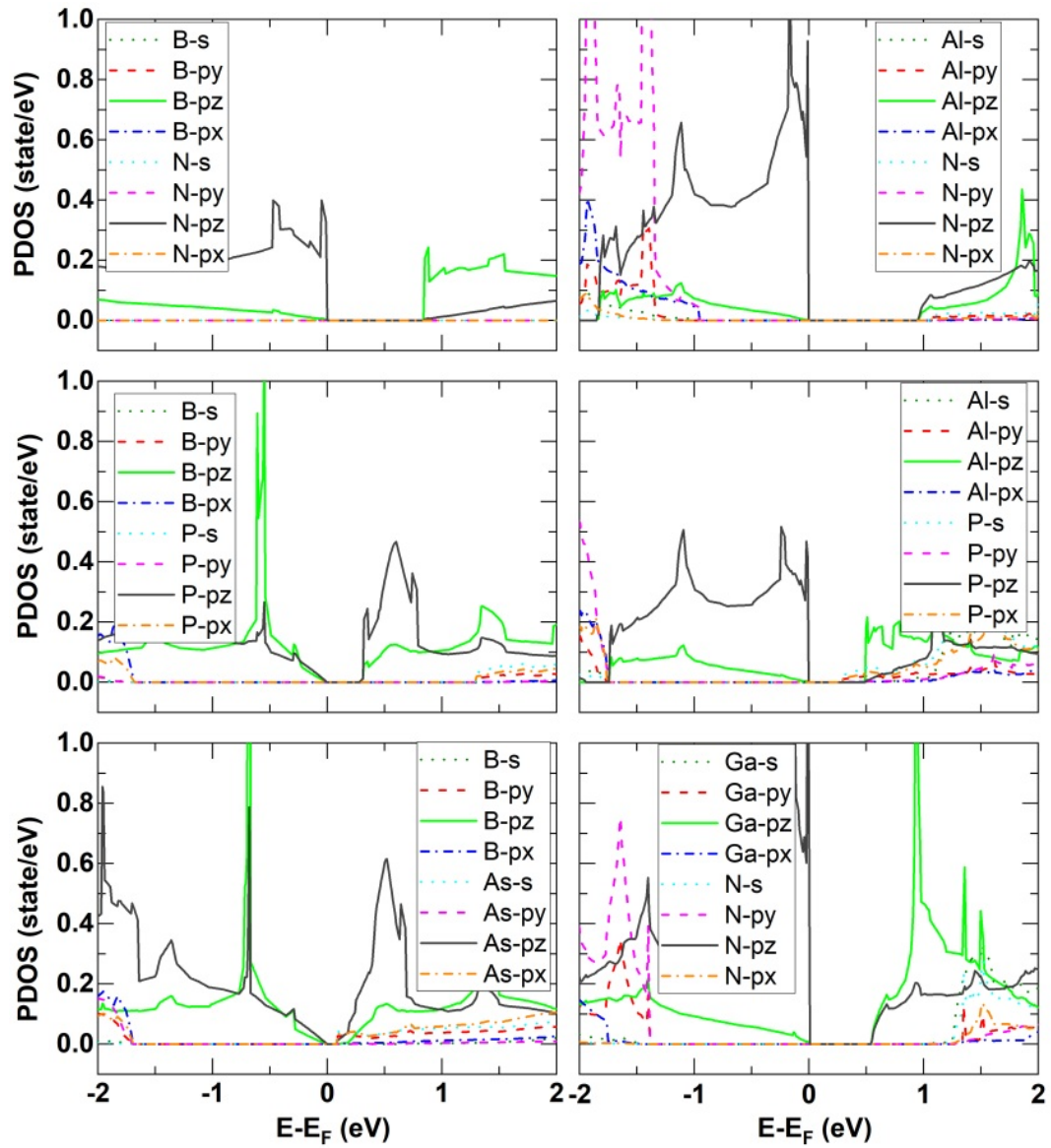


FIG. S14 The calculated GGA-PBE results of the projected density of states (PDOS) of the 2D III-V orthorhombic monolayers.



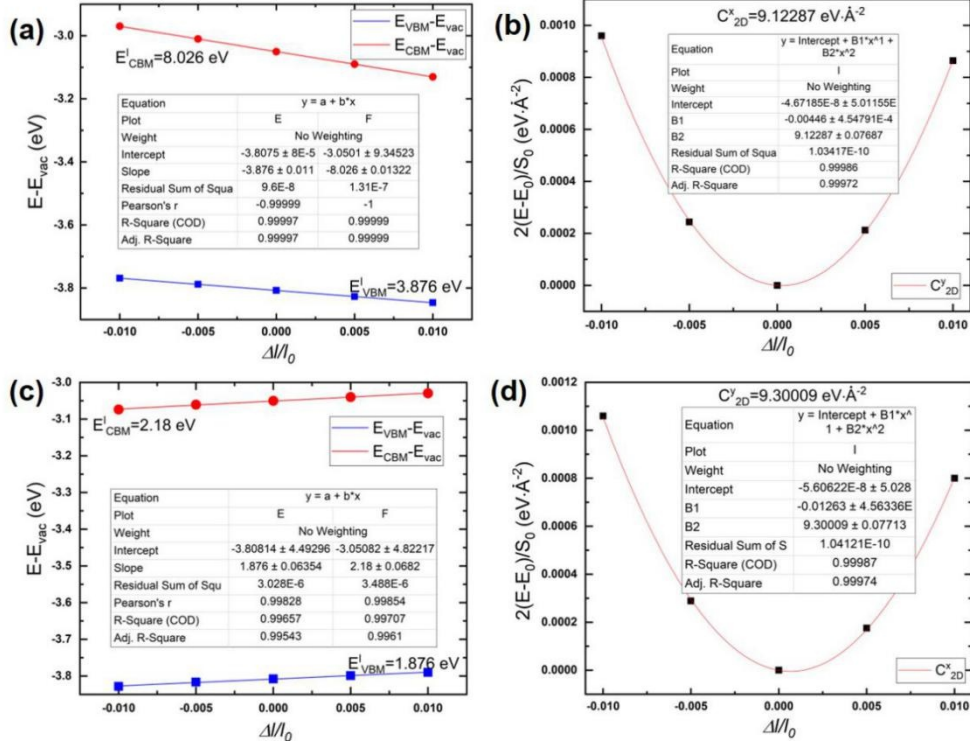


FIG. S15 The deformation potential constants (a, c) and elastic modules (b, d) of the 2D orthorhombic AlN monolayer. (a) and (b) are fittings along x direction; (c) and (d) are fittings along y direction.

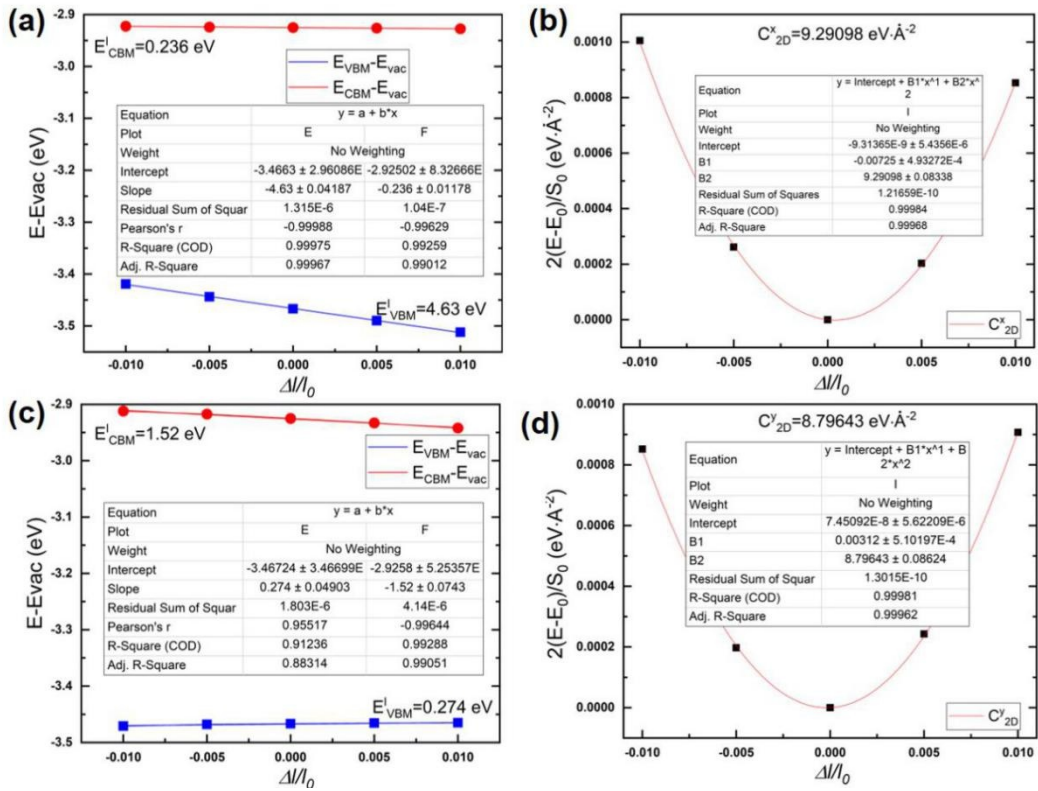


FIG. S16 The deformation potential constants (a, c) and elastic modules (b, d) of the 2D orthorhombic GaN monolayer. (a) and (b) are fittings along x direction; (c) and (d) are fittings along y direction.

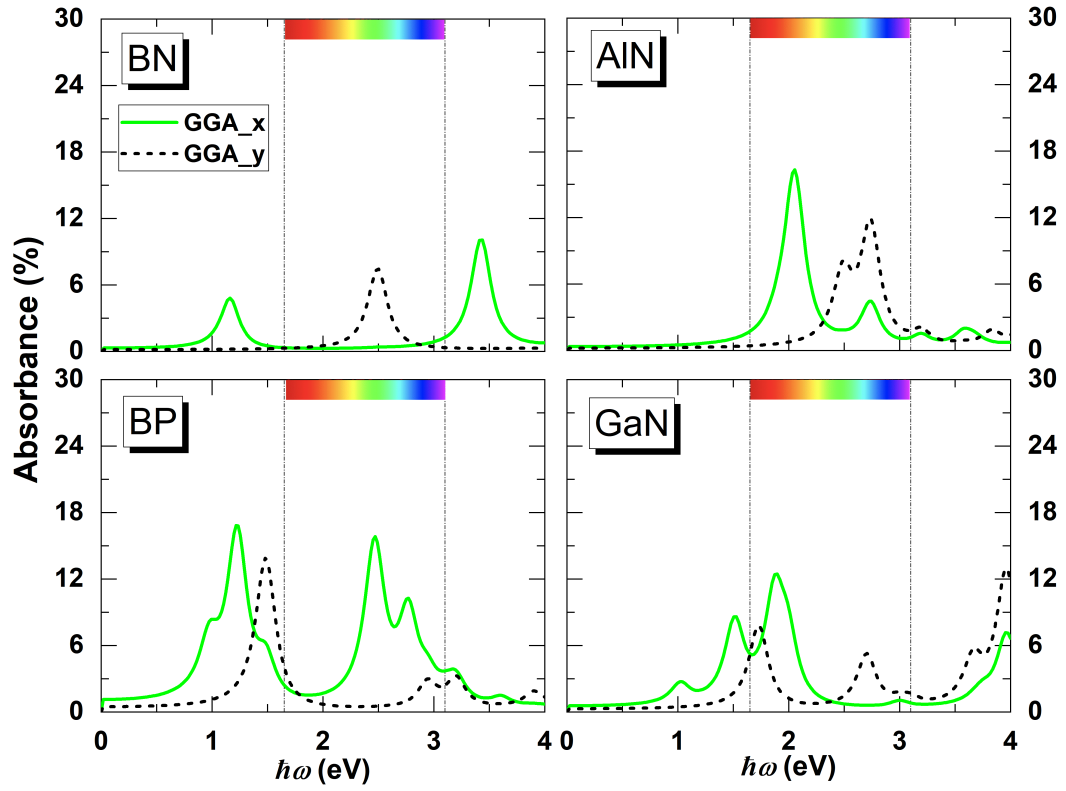


FIG. S17 The direction-dependent optical properties of the absorbance of the 2D III-V orthorhombic semiconductors obtained from GGA-PBE calculations.